Aquatic Toxicology 142–143 (2013) 303–316

Contents lists available at ScienceDirect

Aquatic Toxicology

journal homepage: www.elsevier.com/locate/aquatox

Exxon Valdez to Deepwater Horizon: Comparable toxicity of both crude oils to fish early life stages

John P. Incardona[a,*], Tanya L. Swarts[a], Richard C. Edmunds[a], Tiffany L. Linbo[a], Allisan Aquilina-Beck[a], Catherine A. Sloan[a], Luke D. Gardner[b], Barbara A. Block[b], Nathaniel L. Scholz[a]

[a] Environmental Conservation Division, Northwest Fisheries Science Center, National Oceanic and Atmospheric Administration, 2725 Montlake Boulevard East, Seattle, WA 98112, United States
[b] Stanford University – Hopkins Marine Station, 120 Ocean View Boulevard, Pacific Grove 93950, United States

ARTICLE INFO

Article history:
Received 2 July 2013
Received in revised form 18 August 2013
Accepted 20 August 2013

Keywords:
Oil spills
Fish development
Embryology
Cardiotoxicity
Zebrafish
PAHs

ABSTRACT

The 2010 Deepwater Horizon disaster in the Gulf of Mexico was the largest oil spill in United States history. Crude oils are highly toxic to developing fish embryos, and many pelagic fish species were spawning in the northern Gulf in the months before containment of the damaged Mississippi Canyon 252 (MC252) wellhead (April–July). The largest prior U.S. spill was the 1989 grounding of the Exxon Valdez that released 11 million gallons of Alaska North Slope crude oil (ANSCO) into Prince William Sound. Numerous studies in the aftermath of the Exxon Valdez spill defined a conventional crude oil injury phenotype in fish early life stages, mediated primarily by toxicity to the developing heart. To determine whether this type of injury extends to fishes exposed to crude oil from the Deepwater Horizon – MC252 incident, we used zebrafish to compare the embryotoxicity of ANSCO alongside unweathered and weathered MC252 oil. We also developed a standardized protocol for generating dispersed oil water-accommodated fractions containing microdroplets of crude oil in the size range of those detected in subsurface plumes in the Gulf. We show here that MC252 oil and ANSCO cause similar cardiotoxicity and photo-induced toxicity in zebrafish embryos. Morphological defects and patterns of cytochrome P450 induction were largely indistinguishable and generally correlated with polycyclic aromatic compound (PAC) composition of each oil type. Analyses of embryos exposed during different developmental windows provided additional insight into mechanisms of crude oil cardiotoxicity. These findings indicate that the impacts of MC252 crude oil on fish embryos and larvae are consistent with the canonical ANSCO cardiac injury phenotype. For those marine fish species that spawned in the northern Gulf of Mexico during and after the Deepwater Horizon incident, the established literature can therefore inform the assessment of natural resource injury in the form of potential year-class losses.

Published by Elsevier B.V.

1. Introduction

Crude oils are complex mixtures that contain thousands of different chemicals. Oils from different geological sources differ primarily in the ratios of large and interrelated families of compounds (Stout and Wang, 2007). These include multiple classes of aliphatic hydrocarbons, aromatic hydrocarbons, resins, asphaltenes, and polar compounds containing nitrogen, sulfur or oxygen atoms (NSO compounds). The relative proportions of these compounds determine the general chemical characteristics of a given crude oil. For example, heavier, sulfur-rich crude oils such as Alaska North Slope crude oil (ANSCO) have proportionally more sulfur-containing aromatic heterocycles than the lighter, low-sulfur crude oils from the *Deepwater Horizon* – MC252 well and other South Louisiana formations (Wang et al., 2003). Within crude oil mixtures, toxicity has been attributed primarily to the proportional content of polycyclic aromatic compounds (PACs) and related families of heterocyclic NSO compounds (Carls and Meador, 2009). These chemicals have higher water solubility relative to aliphatic hydrocarbons and polycyclic alkanes, and they are characteristically taken up by oil-exposed organisms (Council, 2003).

Research spanning the past two decades has revealed a common form of injury among teleost embryos exposed to crude oil. Cardiotoxicity is generally the most sensitive phenotype, and this is primarily evident as fluid accumulation (edema) in the pericardial space or yolk sac. This loss of circulatory function and corresponding change in morphology has been documented for several different crude oils, including Alaska North Slope, Mesa light,

* Corresponding author. Tel.: +1 206 860 3347.
E-mail address: john.incardona@noaa.gov (J.P. Incardona).

0166-445X/$ – see front matter. Published by Elsevier B.V.
http://dx.doi.org/10.1016/j.aquatox.2013.08.011

Iranian heavy, and Bass Strait (Couillard, 2002; Incardona et al., 2005; Jung et al., 2013; Pollino and Holdway, 2002) across a range of freshwater and marine species, including mummichog (*Fundulus heteroclitus* (Couillard, 2002)), zebrafish (*Danio rerio* (Carls et al., 2008; Incardona et al., 2005)), rainbowfish (*Melanotaenia fluviatilis* (Pollino and Holdway, 2002)), pink salmon (*Oncorhynchus gorbuscha* (Marty et al., 1997b)), and Pacific herring (*Clupea pallasi* (Carls et al., 1999; Incardona et al., 2009)). Many of the gross morphological features of the crude oil cardiac toxicity syndrome can be attributed to secondary consequences of reduced circulatory function or heart failure (Incardona et al., 2004). Weathering studies previously showed that aliphatic or volatile monoaromatic compounds are not required to produce this cardiovascular syndrome (Marty et al., 1997b). In the zebrafish model, similarities in phenotype between oil-exposed embryos and embryos with a genetic loss of cardiac function led to the discovery that the most abundant classes of PACs in crude oil, the tricyclic fluorenes, dibenzothiophenes and phenanthrenes, are cardiotoxic (Incardona et al., 2004, 2005). Certain crude oils also cause additional morphological defects that are unrelated to PAC cardiotoxicity, including pectoral and caudal fin blisters in response to ANSCO exposure (Incardona et al., 2005) and tail bud defects in response to Iranian heavy crude oil exposure (Jung et al., 2013). Nevertheless, numerous dose–response studies have consistently shown that the developing fish heart is a key target organ for toxicity across crude oil types, and that cardiac effects are the most sensitive indicators of adverse impacts following both lab and field exposures (Carls et al., 1999, 2008; Hicken et al., 2011; Incardona et al., 2012a, 2012b).

Due largely to the scale of the 1989 *Exxon Valdez* oil spill disaster in Alaska's Prince William Sound, ANSCO has been by far the most intensively assessed crude oil in subsequent years, with numerous studies documenting both acute and long-term effects of embryonic exposure in fish (Carls et al., 1999, 2008; Heintz, 2007; Heintz et al., 1999; Hicken et al., 2011; Incardona et al., 2005, 2009; Marty et al., 1997a, 1997b). The more recent and much larger *Deepwater Horizon* spill in the northern Gulf of Mexico exposed embryos and larvae from a wide diversity of fish species to Mississippi Canyon (MC252) crude oil at varying states of weathering. To address whether MC252 produces canonical cardiac injury in fish early life stages, we used the zebrafish model to directly compare the toxicity of ANSCO alongside several types of unweathered and weathered MC252 oil.

We also developed a standardized protocol for producing oiled water-accommodated fractions (WAFs) that more closely emulate the dispersion of oil droplets under high pressure, as occurred during the *Deepwater Horizon* incident. Previous studies have largely reproduced environmentally relevant exposures to surface spills from ships and other sources. Standardized protocols exist for preparation of low-energy WAFs that model a surface spill; e.g., the method developed through the Chemical Response to Oil Spills: Ecological Effects Research Forum (CROSERF (Singer et al., 2000)). However, these procedures do not entrain oil droplets into the water column, and they produce a dissolved hydrocarbon profile dominated by monoaromatics and 2-ring PACs (e.g., naphthalenes). For example, the CROSERF method using Mesa light crude oil shifted the ratio of alkyl-naphthalenes to alkyl-phenanthrenes from approximately 8:1 in source oil to 60:1 in the WAF (Couillard et al., 2005). We and others have previously demonstrated that high-energy (HE)WAF protocols designed specifically to physically disperse small droplets of crude oil result in more weathered patterns dominated by 3-ring PACs (e.g., 2:1 ratio of alkyl-naphthalenes to alkyl-phenanthrenes) (Barron et al., 2003; Incardona et al., 2005). However, these methods used specialized equipment and procedures that are not readily available or standardized. We therefore established a simple method that generates weathered-pattern HEWAFs from dispersed oil droplets with high reproducibility using commercially available equipment. This method allowed for a systematic assessment of the toxicity of MC252 crude oil following dispersion into droplets under high energy, as occurred in the Gulf of Mexico during release of oil from the damaged wellhead or remixing of oil accumulated at the sea surface during high energy conditions.

2. Materials and methods

2.1. Oil samples

MC252 samples were collected by NOAA personnel in cooperation with BP during the active spill phase and transferred under chain of custody to NOAA scientists at the Northwest Fisheries Science Center (Seattle, WA). These included three different weathered samples from surface skimmers (MC252 skim 1, 2, and 3 oils) and unweathered (source) oil obtained from the riser pipe (MC252 riser oil, sample 072610-03) prior to capping of the well. Skim 1 (sample NSR570-A-1) was collected 12 May 2010 from a skimmer working offshore that had just returned to port. Skim 2 (sample CTC02404-02) was collected 29 July 2010 from a barge holding mixed oil offloaded from a number of different skimmers. Skim 3 (sample GU2888-A0719-OE701) was collected from a skimming transect completed 19 July 2010 by the U.S. Coast Guard Cutter *Juniper*. MC252 riser oil (sample 072610-W-A) was artificially weathered by heating with gentle mixing to 90–105 °C until the mass was reduced by 33–38%. ANSCO was from a previously studied stock that was weathered similarly, except heated to 60 °C until the mass was reduced by 20%. This weathering process nearly eliminated monoaromatic compounds and yielded a modest reduction of naphthalenes in the PAC fraction (Carls et al., 2008; Hatlen et al., 2010; Hicken et al., 2011; Incardona et al., 2005).

2.2. Preparation of water accommodated fractions (HEWAFs)

Two methods were used to prepare high energy HEWAFs. Small-volume (<1 L) HEWAFs were prepared by manual shaking in 500-mL or 1-L glass separatory funnels as described previously (Carls et al., 2008; Hatlen et al., 2010). Larger volume HEWAFs were prepared in a 3-speed commercial food blender with a 1-gal (3.8-L) stainless steel container (Waring CB15, Waring Commercial, Torrington, CT). A blender protocol was developed to produce a distribution of oil droplets/particles that was microscopically similar to the manual method. For each preparation, the stainless steel container was cleaned with acetone and dichloromethane, the rubber lid was lined with dichloromethane-rinsed heavy-duty aluminum foil and the container was filled with 2 L of the artificial fresh water used to maintain a zebrafish husbandry facility at the Northwest Fisheries Science Center (system water). DWH-MC252 riser oil was measured and delivered with a positive displacement pipette onto the surface of the system water in the blender container. The surface-collected skim samples were each a highly viscous mousse and were delivered by weight. A target mass was weighed onto a Teflon sheet and loaded onto the water surface by scraping. Delivered mass was calculated by re-weighing the Teflon sheet. Subsequent HEWAFs with surface samples were made by delivering oil volumetrically with a positive displacement pipette following brief (<5 min) heating at 60 °C to increase fluidity.

Water and oil were blended on the lowest speed (30 s for MC252 riser oil and 2 min for the more viscous surface slick samples) and then 1 L was poured into a 1-L separatory funnel. 200–400 mL were transferred to brown glass bottles and stabilized with 20 mL dichloromethane for analysis of PACs (prefilter sample). After sitting for 1 h to allow surface slick formation, the HEWAF was drained from the separatory funnel (with retention of the slick and ~100 mL

HEWAF). To characterize dissolved PACs biologically and chemically, an initial series of HEWAFs were filtered through 2.7 and 0.7 μm glass microfiber filters (GF/D and GF/F, respectively, Whatman/GE Healthcare, Piscataway, NJ) held in a glass filter holder apparatus (VWR International, Radnor, PA). Unfiltered and filtered HEWAFs were immediately divided into 200–400 mL samples for PAC analysis and aliquots for zebrafish embryo exposures. Initial HEWAF preparations included clean controls in which zebrafish system water was blended without oil, transferred to a separatory funnel, and filtered. No difference was observed between these mock-blended negative controls and unprocessed system water, so subsequent experiments included unprocessed system water as a negative control.

2.3. Zebrafish embryo exposures, morphological assessments and imaging

Embryos of zebrafish AB strain were obtained from adults maintained using conventional zebrafish animal care protocols (Linbo, 2009). Embryos were exposed at either 4–6 h (sphere to shield developmental stage) or 28–30 h post-fertilization (hpf). In general, embryos were exposed in replicate groups of 3 or 6 using either 60- or 100-mm glass Petri dishes ($n = 25$ or 35 embryos per replicate, respectively). Cleaned and sorted embryos were transferred to dishes via controlled-drop Pasteur pipettes in small volume of water (<1 mL). The Petri dishes were then filled with 25-mL aliquots of HEWAF, and HEWAFs were not renewed for the duration of exposures. All embryos were screened for abnormalities at 48 hpf, with digital still images and videos collected using a SPOT imaging system (Diagnostic Instruments, Inc., Sterling, MI; camera model 2.3.1; software version 4.5.9.9) or Fire-i 400 camera (Unibrain, San Ramon, CA) fitted to a Nikon SMZ800 stereomicroscope or Nikon Eclipse E600 compound microscope. In some experiments, embryos were incubated to 72 hpf for further morphological characterization. Presence/absence scores for pericardial edema were based on observations in live embryos or digital video clips. The presence of edema was scored as a lack of external epidermal pulsation adjacent to the heart (i.e., no movement of pericardial sac across contractions). Intracranial hemorrhage was scored visually in either live embryos or in lateral images and video clips. For quantification of pericardial edema and detailed imaging, embryos were mounted in 2% methylcellulose. Pericardial area was measured in still frames extracted from digital video as described previously (Incardona et al., 2006). For cardiac dimensional measurements, embryos were mounted without anesthesia in 2% methylcellulose and digital video collected using differential interference contrast optics with a 20× objective lens on the Nikon E600 compound microscope. Diastolic and systolic chamber diameters were measured and fractional shortening (contractility) as described elsewhere (Bendig et al., 2006; Incardona et al., 2011). For caudal finfold measurements, embryos were exposed from 4 to 72 hpf in unfiltered HEWAF in 3 replicates (25 embryos in 20 ml). 10 larvae were randomly selected from each replicate, anesthetized with MS-222, and mounted in 2% methylcellulose for imaging. Using ImageJ area measurements were taken by tracing a roughly half-circular line using the end of the notochord as a landmark along the posterior edge of the caudal finfold.

For assessment of morphological defects in exposed juveniles, six replicate groups of 35 embryos each were exposed from shortly after fertilization (4–6 hpf) through 48 hpf and then scored for pericardial edema. HEWAF-exposed embryos were then pooled and re-divided into three replicate groups ($n = 30$ each) with edema and three replicate groups ($n = 30$ each) without edema. In control embryos, rates of edema were low enough to provide only a single group with edema ($n = 30$), while embryos without edema were pooled into five replicate groups ($n = 30$ each). The new replicate groups were transferred to clean water, incubated at 28.5 °C in 100-mm Petri dishes until feeding stage and then raised until juvenile stage (2 weeks post-fertilization) as detailed elsewhere (Linbo, 2009), with mortality assessed daily. At 2 weeks post-fertilization, fish were anesthetized, assessed for morphological defects, and lengths measured. Representative individuals were imaged. A subset of individuals from each treatment was randomly selected, fixed and assessed for craniofacial skeletal defects as described below.

Phototoxicity tests were carried out after exposing embryos to HEWAFs from 4 to 72 hpf as detailed previously (Hatlen et al., 2010). Briefly, embryos were exposed to ANSCO or skim 1 HEWAFs (prepared manually), or AW-riser blender HEWAFs in a dark laboratory incubator from 4 to 72 hpf, transferred into new Petri dishes with clean water, exposed outdoors to full sunlight for 30 min and then returned to the laboratory for immediate imaging. Sunlight exposure was carried out 2 July 2010 at 2:30 PM under partly cloudy skies at an ambient temperature of 20 °C, and on 10 May 2013 under clear skies at 25.5 °C. UVA dose recorded for the second (May 2013) exposure was 15,410 mW/m^2 over 30 min. UV levels were measured with a Macam UV203 radiometer (Advanced Photonics International, Inc., Fairfield, CT) set on average mode for the duration of the sunlight exposure.

2.4. Analysis of craniofacial skeletal structure in juveniles

Following morphometric data collection, fish were fixed in 4% paraformaldehyde overnight at 4 °C on a rocker, dehydrated through a gradient of methanol/phosphate–buffered saline (PBS) (25%/75%, 50%/50%, 75%/25%; 5 min each) and stored at −20 °C in 100% methanol. For staining, samples were rehydrated through methanol/PBS series (75%/25%, 50%/50%, 25%/75%; 10 min each) and washed in water (3 times; 1 hr each). Fish were then stained with alcian blue solution (0.01% in 7:3 ethanol/glacial acetic acid; 24 h), destained (7:3 ethanol/glacial acetic acid; 30 min), transferred into 100% EtOH (30 min), rehydrated through ethanol/water series (75%/25%, 50%/50%, 25%/75%; 30 min each) and washed in water (2 times; 30 min each). Following rehydration, alcian stained fish were subjected to trypsin digestion (50% saturated aqueous sodium borate, 1.7% trypsin powder; 10 min) before 0.5% KOH enzyme deactivation (5 min) and 0.5% KOH washes (2 times; 5 min each). Alizarin Red S solution (0.04%) was added to samples (in 0.5% KOH) until solution turned deep purple. Alizarin staining proceeded for 12 h before clearing through 0.5% KOH/glycerol series (3:1, 1:1, 1:3; 6 h each) and storage in 100% glycerol. Dissected craniofacial skeletons were mounted in glycerol and imaged using the Nikon Eclipse E600 compound microscope and SPOT imaging system. Multiple images encompassing all focal planes ($n = 10$) were then aligned and Z-stacked using Hugin version 2011.4.0 (http://hugin.sourceforge.net/) and Enfuse version 4.0 (http://enblend.sourceforge.net/) to generate an extended depth of field.

2.5. Analytical chemistry

Water samples were stored in brown glass bottles containing 20 mL dichloromethane until analysis for PACs and phytane. For quality assurance, a blank water sample (control) and a spiked blank were prepared in brown glass bottles, both containing 200 or 345 mL of zebrafish system water and 20 mL of dichloromethane along with known solutions of selected PACs (34 ng of each analyte) and phytane (200 ng) added to the spiked blank. After the addition of surrogate standards (340 ng each of D8-naphthalene, D10-acenaphthene and D12-benzo[*a*]pyrene in 200 μL of isooctane), each sample was transferred to a 1-L separatory funnel. Samples were extracted by shaking with dichloromethane for 2 min followed by 2 min separation time. After collecting the

dichloromethane phase, samples were extracted a second time with another 20 mL of dichloromethane and the two extracts were combined. Sodium sulfate (20 g) was added to each sample and left to sit overnight. The extracts were cleaned up using gravity-flow silica/alumina columns as previously described (Sloan et al., 2005) then exchanged from dichloromethane to isooctane while being concentrated to 200–1000 μL, depending on the expected PAC concentrations. D10-phenanthrene (295 ng in 200 μL of isooctane) was added as an internal standard to determine the recovery of surrogate standards.

To quantify PACs and phytane, extracts were analyzed using gas chromatography/mass spectrometry (GC/MS) selected ion monitoring as described previously (Sloan et al., 2005) with additional monitoring for alkyl-PACs and phytane. Analyte concentrations in water (μg/L) were calculated using surrogate standards and six concentration levels of GC/MS calibration standards ranging from 0.003 to 1.0 ng/μL. For each analyte, the concentration producing the peak response in the lowest level calibration standard was used to calculate the lower limit of quantitation (LOQ). LOQs ranged from approximately 0.004 to 0.02 μg/L. Surrogate standard recoveries ranged from 90 to 108% and the spiked blank recoveries ranged from 89 to 104%. The control water samples contained 0.047–0.17 μg/L total low molecular weight PACs, whereas the high molecular weight PACs in these samples were <LOQ – 0.03 μg/L.

2.6. Statistical analysis

Statistical test were carried out with either JMP 6.0.2 or JMP 8.0.1 for Macintosh (SAS Institute, Inc., Cary, NC). Tests that involved measures in individual embryos from replicate groups (e.g., pericardial area, caudal finfold area, fractional shortening) were subjected to ANOVA with replicate nested in treatment to avoid pseudoreplication. Edema occurrence data were analyzed by one-way ANOVA with post hoc means comparisons performed using Tukey–Kramer Honestly Significant Differences test ($\alpha = 0.05$). For measures of edema severity using pericardial area, both MC252 riser oil dose-dependency and multiple oil comparison assays presented a significant replicate or "tank" effect. However, this was due to overlapping levels of severity at higher oil loadings or $\sum$PAC concentrations. For fractional shortening (contractility) measures, there was no replicate effect ($P = 0.3$).

3. Results

3.1. Generation of HEWAFs and analysis of PACs

MC252 oil is a lighter weight crude (American Petroleum Institute [API] gravity 37) with lower sulfur content than the medium weight ANSCO (API gravity 30). This difference in sulfur content is reflected in the lower concentrations of dibenzothiophenes in MC252 riser oil (Fig. 1A). Concentrations of the other more abundant PACs (naphthalenes, fluorenes and phenanthrenes) were very similar between MC252 riser oil and ANSCO, while ANSCO had slightly higher concentrations of chrysenes. Increased weathering was evident in MC252 skim 1 and skim 2 samples (Fig. 1A), with respective losses of naphthalenes by 72% and 90%, fluorenes by 55% and 51%, dibenzothiophenes by 48% and 42%, and phenanthrenes by 48% and 45%. Therefore, the largest differences between unweathered riser oil and weathered samples skimmed from the ocean surface were in the concentrations of naphthalenes, which are not major contributors to crude oil toxicity at fish early life stages (Carls et al., 1999; Heintz et al., 1999; Incardona et al., 2004). Artificially weathered (AW) riser oil was comparable to skim 1, whereas MC252 skim 3 was the most highly weathered, with an additional depletion of naphthalenes (Fig. S1).

Supplementary data associated with this article can be found in the online version, at http://dx.doi.org/10.1016/j.aquatox.2013.08.011.

Initial characterization of MC252 skim 1 toxicity (described below) used small-scale, manually produced high-energy HEWAFs (Carls et al., 2008; Hatlen et al., 2010), for which PACs were not measured. Three independent HEWAFs were prepared with the same loading of MC252 riser oil to standardize the blender method (Fig. 1B). Microscopic examination showed a distribution of oil droplets/particles similar to that derived from the manual method (Carls et al., 2008), generally ≤10 μm (Fig. S2). Environmentally realistic tests of MC252 oil toxicity should include both oil droplets and dissolved PACs, and we therefore characterized filtered and unfiltered HEWAFs to determine the reproducibility of the method for generating WAFs with dissolved (i.e., bioavailable) PACs. Analysis of unfiltered HEWAF showed a distribution of PACs that corresponded closely with the whole oil (Fig. 1B, black bars; compare to black bars in Fig. 1A). Filtration of the HEWAF through 2.7 and 0.7 μm glass fiber filters removed particulate oil by 96%, as evidenced by a reduction in phytane concentration from 22.7 ± 0.9 to 1.0 ± 0.1 μg/L (Fig. 1B, inset). The dissolved, aqueous-phase PACs were dominated by the more soluble naphthalenes and tricyclic compounds, with very little contribution from chrysenes and other 4-ringed PACs (Fig. 1B, gray bars). In one experiment (results described below), embryos were exposed to a fourth unfiltered HEWAF with a PAC profile essentially identical to the average obtained during method development (Fig. 1C), indicative of technical reproducibility. The concentrations of dissolved aqueous PACs in this fourth HEWAF were assumed to be the same as the average PAC concentrations in filtered HEWAFs, based on the measured dissolved/particulate $\sum$PAC ratio of 0.46 ± 0.01 (Fig. 1B).

Supplementary data associated with this article can be found in the online version, at http://dx.doi.org/10.1016/j.aquatox.2013.08.011.

We also prepared HEWAFs with the more viscous MC252 skim (surface) samples using the blender method. After filtration, dissolved aqueous PACs showed a more weathered pattern consistent with the differences between the MC252 riser and skim oil samples (Fig. 1D). Overall, HEWAFs from MC252 riser and skim samples contained similar concentrations of tricyclics ($\sum$TACs; 20.0 ± 0.4 and 18 ± 2 μg/L, respectively; $P_{ttest} = 0.27$). However, MC252 skim 2 HEWAF had much lower concentrations of naphthalenes (15.8 ± 1.8 vs. 147.4 ± 5.9 μg/L; $P_{ttest} = 0.0009$) and higher (but still very low) concentrations of chrysenes (1.5 ± 0.1 vs. 0.4 ± 0.2 μg/L; $P_{ttest} = 0.02$). Notably, MC252 skim 2 HEWAF had almost 4× and 2.5× lower concentrations of parent fluorene (F0, 0.7 ± 0.1 vs. 2.6 ± 0.1 μg/L; $P_{ttest} = 0.02$) and phenanthrene (P0, 1.4 ± 0.3 vs. 3.36 ± 0.03 μg/L; $P_{ttest} = 0.09$), respectively (Fig. 1D). Compositional differences among various MC252 oil samples were also observed in subsequent HEWAF preparations using the blender method (Fig. S3, Table 1). These compositional differences corresponded with the cardiotoxic potency of a given sample (see below).

Supplementary data associated with this article can be found in the online version, at http://dx.doi.org/10.1016/j.aquatox.2013.08.011.

3.2. Weathered MC252 oil and ANSCO produce similar gross morphological defects and phototoxicity

We used exposures of zebrafish embryos to biologically characterize the two types of oil (MC252 and ANSCO). MC252 skim 1 was a water-in-oil emulsification or mousse with roughly 3× lower $\sum$PAC concentrations per unit mass relative to ANSCO. We therefore initially exposed zebrafish embryos to manually prepared HEWAFs (see Material and Methods above) loaded with masses of

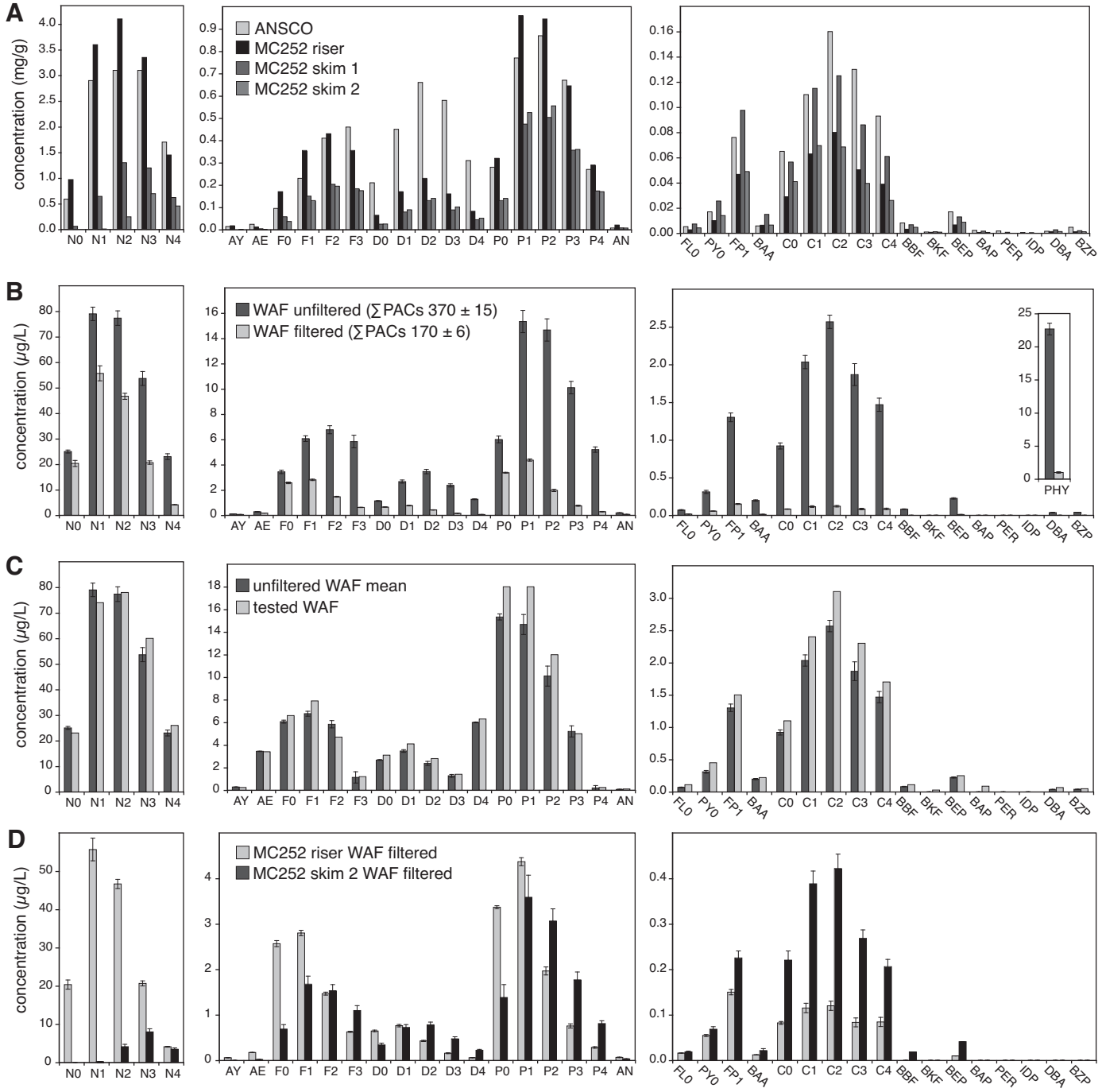

Fig. 1. PAC concentrations in oils and HEWAF preparations. Molecular weight increases to the right with separate *y*-axes for naphthalenes (left), 3-ring (middle) and 4- to 6-ring compounds (right). (A) Concentrations in whole oils. A single measurement was performed for each oil; bars represent left to right, ANSCO, MC252 riser, MC252 skim 1, MC252 skim 2. (B) Filtered (black bars) and unfiltered (gray bars) MC252 riser HEWAF (50 ppm nominal oil load). Inset in right panel shows phytane (PHY). Data are mean ± SEM from three independent HEWAF preparations. (C) Data from average unfiltered 50 ppm MC252 riser HEWAFs (black bars) shown in (B) compared to unfiltered 50 ppm MC252 riser HEWAF (gray bars) used for quantification of pericardial edema shown in Fig. 6. (D) Data from filtered MC252 riser HEWAF shown in (B, gray bars) compared to filtered 50 ppm MC252 skim 3 HEWAF (mean ± SEM, $N = 2$) linked to toxicity data in Table 2. N, naphthalenes; AY, acenaphthylene; AE, acenaphthene; F, fluorene; D, dibenzothiophene; P, phenanthrene; AN, anthracene; FL, fluoranthene; PY, pyrene; FP, fluoranthenes/pyrenes; BAA, benz[*a*]anthracene; C, chrysene; BBF, benzo[*b*]fluoranthene; BKF, benzo[*j*]fluoranthene/benzo[*k*]fluoranthene; BEP, benzo[e]pyrene; BAP, benzo[a]pyrene; PER, perylene; IDP, indeno[1,2,3-*cd*]pyrene, DBA, dibenz[*a,h*]anthracene/dibenz[*a,c*]anthracene; BZP, benzo[*ghi*]perylene. Parent compound is indicated by a 0 (e.g., N0), while numbers of additional carbons (e.g. methyl groups) for alkylated homologs are indicated as N1, N2, etc.

ANSCO and MC252 skim 1 samples predicted to yield similar aqueous PAC concentrations. Initial exposures were performed in a dark incubator, and the toxic effects of ANSCO and MC252 skim 1 on the gross morphology of embryos were indistinguishable (Fig. 2B and C). For example, exposure to MC252 oil produced conventional signs of canonical petrogenic PAC cardiotoxicity as characterized by concentration-dependent pericardial edema (Fig. 2B and C), cardiac dysfunction (e.g., atrial regurgitation) and poor cardiac looping observed by failure of the atrioventricular canal to adopt a lateral orientation (Fig. 3; Movie S1). Notably, cardiac phenotypes were essentially identical in embryos exposed either shortly after fertilization (Fig. 3B) or starting at 24 hpf (Fig. 3C) when the initial

Table 1
Compositional differences between MC252 oil sample high-energy water-accommodated fractions (HEWAFs) at 50 ppm oil loads.[a]

Oil[b]	∑NPHs[c] (μg/L)	∑TACs (μg/L)	∑parent TACs (μg/L)	∑alkyl TACs (μg/L)	% parent TACs
Riser	147	20	6.6	13.7	32
Skim 2	10.3	9.2	2	7.2	21
Skim 3	2.0	14.8	0.9	13.9	6.1

[a] Toxicity data for these HEWAFs are shown in Fig. 7.
[b] Oil samples are riser, unweathered oil collected from the wellhead; skim 2, surface slick oil collected July 29, 2010; skim 3, surface slick oil collected July 19, 2010.
[c] ∑NPHs, sum of parent and alkyl-naphthalenes; ∑TACs, sum of non-alkylated and alkylated tricyclic compounds, i.e., fluorenes, dibenzothiophenes, and phenanthrenes; ∑parent TACs, sum of non-alkylated tricyclic compounds; ∑alkyl TACs, sum of alkylated tricyclic compounds; % parent TACs, percent of non-alkylated compounds out of total tricyclic compounds.

heart tube is already beating and providing circulation (detailed below). In addition, a high percentage of embryos demonstrated intracranial hemorrhage (Fig. 2A′–C′). Hemorrhages were transient and occurred between 30 and 44 hpf; normal blood flow through the cerebral vasculature was typically observed in embryos with intracranial hemorrhage, with no erythrocytes visibly contributing to hemorrhages by 48 hpf (data not shown). The dose–response relationship for edema (Fig. 2D) was much more similar for the two oils than the relationship for intracranial hemorrhage (Fig. 2E). Although MC252 crude oil appeared to be about 3-times more potent than ANSCO based on nominal oil loads, the MC252 skim 1 sample was an oil-water emulsion that contained about 3-times less total PACs than the artificially weathered ANSCO.

Supplementary data associated with this article can be found in the online version, at http://dx.doi.org/10.1016/j.aquatox.2013.08.011.

As observed previously for similar ANSCO HEWAF preparations (Hatlen et al., 2010), outgrowth of finfolds was reduced following exposure to both oils (Fig. 4, S4). Although we did not quantify this defect for the MC252 skim 1 exposure, this sample of MC252 oil appeared to have a slightly more pronounced effect on finfold growth than ANSCO (Fig. S4). In a dose-response series with AW-riser oil HEWAF made using the blender method, finfold growth was significantly reduced (to 87% of control; $P = 0.0003$) at only the highest tested concentration (100 ppm whole oil; Fig. 4A). There were no signs of morphological toxicity to other organ systems.

Supplementary data associated with this article can be found in the online version, at http://dx.doi.org/10.1016/j.aquatox.2013.08.011.

To determine if there were morphological defects that persisted after a transient exposure during embryogenesis, zebrafish were subsequently raised in clean water for 14 days for examination

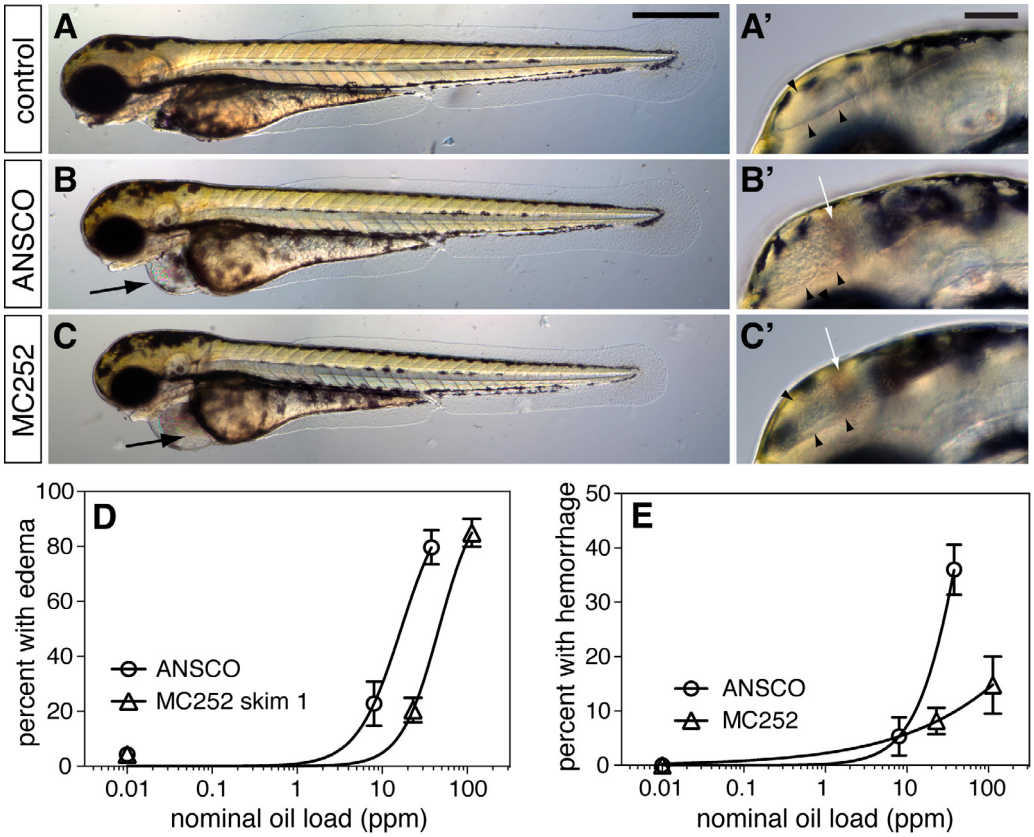

Fig. 2. Gross morphology of zebrafish embryos at 72 hpf (hatching stage) following oil exposure and sequential oil and sunlight exposure. Embryos were exposed to (A) clean water in dark incubator, (B) ANSCO high dose in dark incubator, (C) MC252 skim 1 high dose in dark incubator. Arrows in (B) and (C) indicate pericardial edema. (A′–C′) Midbrain/hindbrain regions are shown with anterior to left. Arrowheads indicate the margins of the midbrain ventricle, and white arrows indicate red tinge from erythrocytes within the midbrain ventricle. Scale bars are 0.5 mm (A–C) and 50 μm (A′–C′). Dose-dependent occurrence of (D) pericardial edema and intracranial hemorrhage (E) in embryos exposed to either ANSCO (○) or MC252 skim 1 (△) HEWAFs. Data are mean ± s.e.m. of 3 replicates (22–25 embryos each).

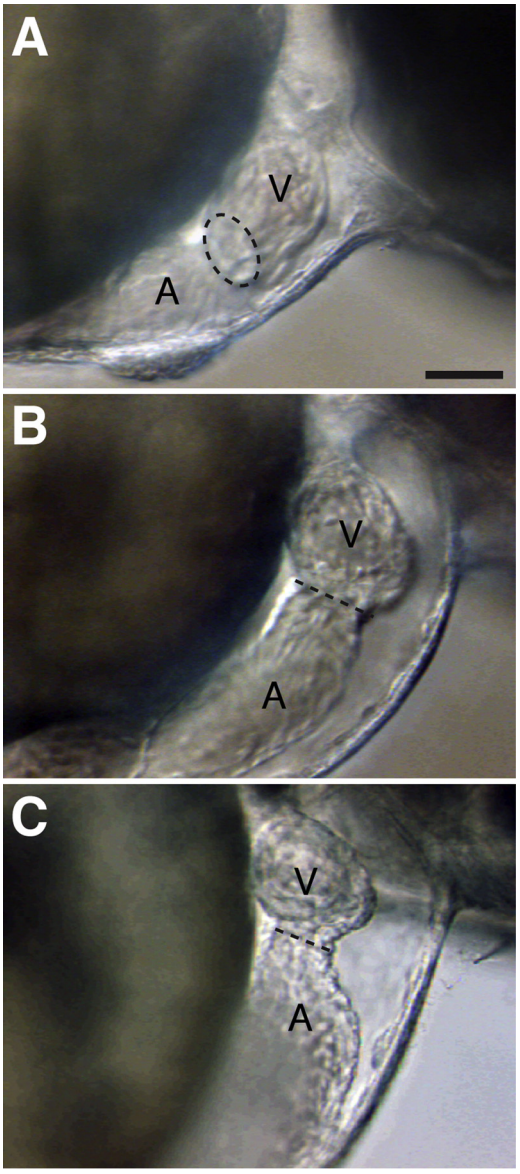

Fig. 3. Poor cardiac looping in MC252-exposed embryos. Embryos were exposed to artificially weathered MC252 riser oil from 4 to 48 hpf, mounted in methylcellulose, and imaged with digital video on a compound microscope. Images show a single video frame captured during ventricular diastole in control (A) and embryos exposed to MC252 crude oil from either 4 to 48 hpf (B), or 28 to 48 hpf (C). Anterior is to the right and dorsal at top, with the right side of the embryo viewed to focus on the ventricle more clearly. Dashed lines indicate the atrioventricular canal. *A*, atrium; *V*, ventricle. Scale bar is 50 μm.

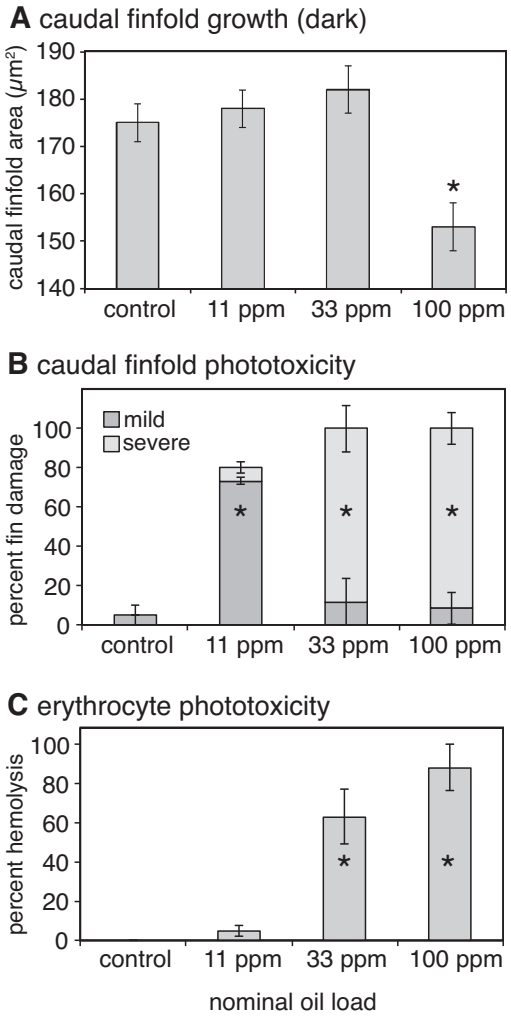

Fig. 4. Reduction of caudal finfold growth by MC252 oil exposure and phototoxic damage to finfold tissue and erythrocytes following subsequent sunlight exposure. (A) Caudal finfold tip area in embryos exposed to MC252 AW-riser oil. Data represent mean ± s.e.m. from 3 replicates (10 embryos each). ANOVA (replicate nested in treatment) showed a significant effect of oil exposure ($P = 0.0001$) but no replicate "tank" effect ($P = 0.6$). (B) Incidence of caudal finfold disruption characterized by a binary score of mild or severe. (C) Incidence of photoinduced hemolysis. Data in (B) and (C) represent mean ± s.e.m. for three replicates of 20 embryos each. ANOVA was significant for effect of oil. Asterisks indicate groups statistically different from controls identified by a post hoc Dunnett's test ($\alpha = 0.05$).

as juveniles. Embryos were exposed shortly after fertilization to MC252 skim 2 HEWAF prepared with 33 ppm nominal oil load predicted to have a dissolved $\sum$PAC of approximately 110 μg/L. At 48 hpf edema was present in 54 ± 2% and 18 ± 3% of oil-exposed and control embryos, respectively (Table 2). After sorting embryos into edematous and non-edematous subgroups and rearing to 14 dpf, oil-exposed animals that had edema at 48 hpf showed elevated mortality relative to oil-exposed embryos without edema ($P = 0.04$). Statistical analysis could not be applied to controls with edema, due to the lower prevalence and single replicate group. In this particular experiment there was a higher than typical level of cardiac abnormalities in controls leading to edema. When placed in larval rearing tanks, embryos with severe edema generally did not feed and died within 9 days, while those with less severe edema survived. Control embryos with edema also showed higher mortality, although the single replicate precluded statistical analysis. The potentially higher relative mortality in controls probably reflects a more severe (e.g., genetic) etiology underlying background cardiac abnormalities. The gross morphology of the control and oil-exposed juveniles that survived was indistinguishable, regardless of whether or not they had edema as embryos (Fig. S5A–D). We also assessed craniofacial development in a subset of each group and found no difference in pharyngeal arch number (i.e., ceratobranchials 1–7 present) or ossification (e.g., pharyngeal teeth present) between oil-exposed and control juveniles (Fig. S5E–H).

Supplementary material related to this article can be found, in the online version, at http://dx.doi.org/10.1016/j.aquatox.2013.08.011.

We also assessed the acute phototoxicity of MC252 oil samples using a previously established protocol (Hatlen et al., 2010) by exposing embryos to HEWAFs, transferring them to clean water, and then exposing them to ambient sunlight. We directly compared the phototoxicity of MC252 skim 1 and ANSCO in a subsample of embryos (3 groups of 10 each) from control and high dose

Table 2
Relationship between embryonic pericardial edema and delayed mortality up to the juvenile stage following MC252 exposure.

	Edema 48 hpf (percent)	Mortality at 14 dpf (percent)	
		Non-edematous	Edematous
Control	18 ± 2.5 (6, 35)[a]	4.0 ± 1.9 (5, 30)	26.7 (1, 30)
Oil-exposed	54.3 ± 2.0 (6, 35)	3.3 ± 1.9 (3, 30)	15.6 ± 4.0 (3, 30)[b]

[a] For each group parentheses indicate number of replicates and embryos per replicate.
[b] Mortality significantly higher than non-edematous oil-exposed fish (*t*-test, $P = 0.04$).

ANSCO (38 ppm oil mass loading) and MC252 (113 ppm) treatments from a cardiotoxicity assessment experiment (e.g., Table 2), and quantified the phototoxicity of AW-riser HEWAF in a second dose–response test. For the skim 1/ANSCO comparison, ultraviolet radiation was not recorded, but compared to previously measured conditions (Hatlen et al., 2010) were estimated to be in the range of 15,000–20,000 mW/m^2. The UV dose was 15,410 mW/m^2 for the AW-riser HEWAF exposure. Control embryos were unaffected by this short sunlight exposure (Fig. S4A, A′), while both ANSCO (Fig. S4B, B′) and MC252 skim 1 (Fig. S4C, C′) produced modest phototoxicity (relative to more potent bunker oils (Incardona et al., 2012b)) in the form of collapsed caudal finfold tissue and hemolysis (Movie S2). Essentially identical results were obtained with AW-riser HEWAF at nominal oil loads of 11, 33, and 100 ppm, which caused both caudal finfold disintegration (Fig. 4B, Fig. S4D–G)) and hemolysis (Fig. 4C) in a concentration-dependent manner. In each experiment, caudal finfold damage and hemolysis were apparent as soon as animals were returned indoors for microscopic examination (i.e., within minutes of terminating sunlight exposure), and worsened in severity over an image acquisition period of about an hour.

Supplementary material related to this article can be found, in the online version, at http://dx.doi.org/10.1016/j.aquatox.2013.08.011.

3.3. Specific aspects of cardiovascular toxicity common to ANSCO and MC252

We quantified the cardiotoxic effects of MC252 oils samples by the occurrence and severity of pericardial edema as observed microscopically. The key developmental period for disruption of cardiac function by petrogenic PACs is approximately 36 hpf (Incardona et al., 2004), when the atrioventricular conduction pathway is forming (Chi et al., 2008). Consistent with this, exposure to MC252 crude oil beginning either shortly after fertilization (4–6 hpf) or after 24 hpf produced characteristic defects in cardiac function (e.g., Incardona et al., 2005; Carls et al., 2008) resulting in pericardial edema by 48 hpf, and effects were essentially identical whether embryos were exposed to filtered HEWAFs or unfiltered preparations containing particulate oil. Filtered HEWAFs with equivalent nominal mass loadings (50 ppm) of MC252 riser oil and MC252 skim 3 had similar levels of total dissolved tricyclic PACs ($\sum$TACs; 21 and 16 μg/L, respectively) and produced similar rates of pericardial edema (52 ± 10% and 42 ± 9%, respectively) in embryos that were exposed from 24 hpf to 48 hpf (Fig. 5A). However, because of higher levels of naphthalenes, $\sum$PACs were much higher for MC252 riser oil HEWAF than the MC252 skim 3 HEWAF (170 μg/L vs. 34 μg/L, respectively; above and Fig. 1D). Embryos exposed to MC252 riser oil displayed erythrocyte regurgitation through the sinoatrial valve at a higher frequency than those exposed to MC252 skim 3 (Fig. 5B). While embryos exposed from shortly after fertilization (4–6 hpf) showed intracranial hemorrhages, this abnormality was notably absent in embryos exposed to either MC252 oil sample beginning at 24 hpf.

We further assessed the dose-dependency of MC252 riser oil cardiovascular toxicity by exposing embryos to unfiltered HEWAFs from 4 to 48 hpf (Fig. 5C, D). In this experiment, edema was quantified by measuring the increase in pericardial area in lateral images of embryos (Incardona et al., 2006). Nominal loadings of 10, 50 and 250 ppm mass oils produced HEWAFs with $\sum$PACs (dissolved plus particulate) of 84, 390, and 470 μg/L, respectively. The concentrations of individual PACs in the 50 ppm loaded HEWAF were the same as the method average determined during protocol development (Fig. 1C) and, based on the average of filtered HEWAFs (filtered to unfiltered $\sum$TACs ratio of 0.24 ± 0.01; Fig. 1B), expected levels of aqueous dissolved $\sum$TACs in the 10, 50, and 250 ppm HEWAFs were 5, 23, and 29 μg/L, respectively. The non-linearity of PAC concentrations at the highest loading is most likely due to larger droplets of oil that were observed adhering to the blender wall, undispersed. Importantly, the severity of pericardial edema (Fig. 5C) and frequency of intracranial hemorrhaging (Fig. 5D) increased with oil dose.

We also directly compared identical mass loadings of high energy HEWAFs for four different MC252 samples and ANSCO in simultaneous exposures (Fig. 6). Consistent with the findings described above for the high energy HEWAF method development, nominal 50 ppm mass loadings of the five different oils produced different PAC concentrations in unfiltered HEWAFs that correlated with sample viscosity and ease of physical dispersion (Fig. S2, Table 1). The more fluid, less-weathered samples (ANSCO, MC252 riser with and without artificial weathering) produced HEWAFs with higher $\sum$PACs and generally more severe cardiotoxicity than the relatively viscous surface slick samples (skims 2 and 3), as measured by either incidence (Fig. 6A) or extent (Fig. 6B) of pericardial edema. Compared to the lower-potency oil–water emulsion samples (e.g., MC252 skim 1, Fig. 2D), the AW-riser oil was more similar to ANSCO. Nevertheless, MC252 riser oil HEWAF was only slightly more cardiotoxic than the weathered samples (e.g., 65 ± 3% edema for riser oil vs. 37 ± 10% edema for skim 3) despite having roughly 10-times higher levels of naphthalenes. For this oil type, however, the frequency of edema appeared to correspond more closely with the percentage of parent TACs than $\sum$TACs (parent plus alkylated forms; Table 1).

Finally, we characterized the effect of exposure to MC252 oil on cardiac function by digital video analysis. Embryos exposed to a HEWAF of MC252 artificially weathered riser oil (100 ppm nominal mass oil load) from 24 to 48 hpf were not different from controls in terms of the dimensions of the atrium during both diastole and systole, nor was there a difference in atrial contractility as measured by fractional shortening (Table 3). In contrast, MC252-exposed embryos had ventricles with significantly reduced diastolic diameters and contractility, but no change in systolic diameter.

3.4. Tissue-specific patterns of CYP1A induction following exposure to MC252 HEWAF

The distribution of CYP1A protein in embryos exposed to MC252 riser oil over durations of 4–48 hpf was assessed by immunofluorescence and confocal microscopy (Fig. 7). Unexposed control embryos showed background levels of CYP1A expression in the form of relatively weak immunofluorescence in vascular endothelium and

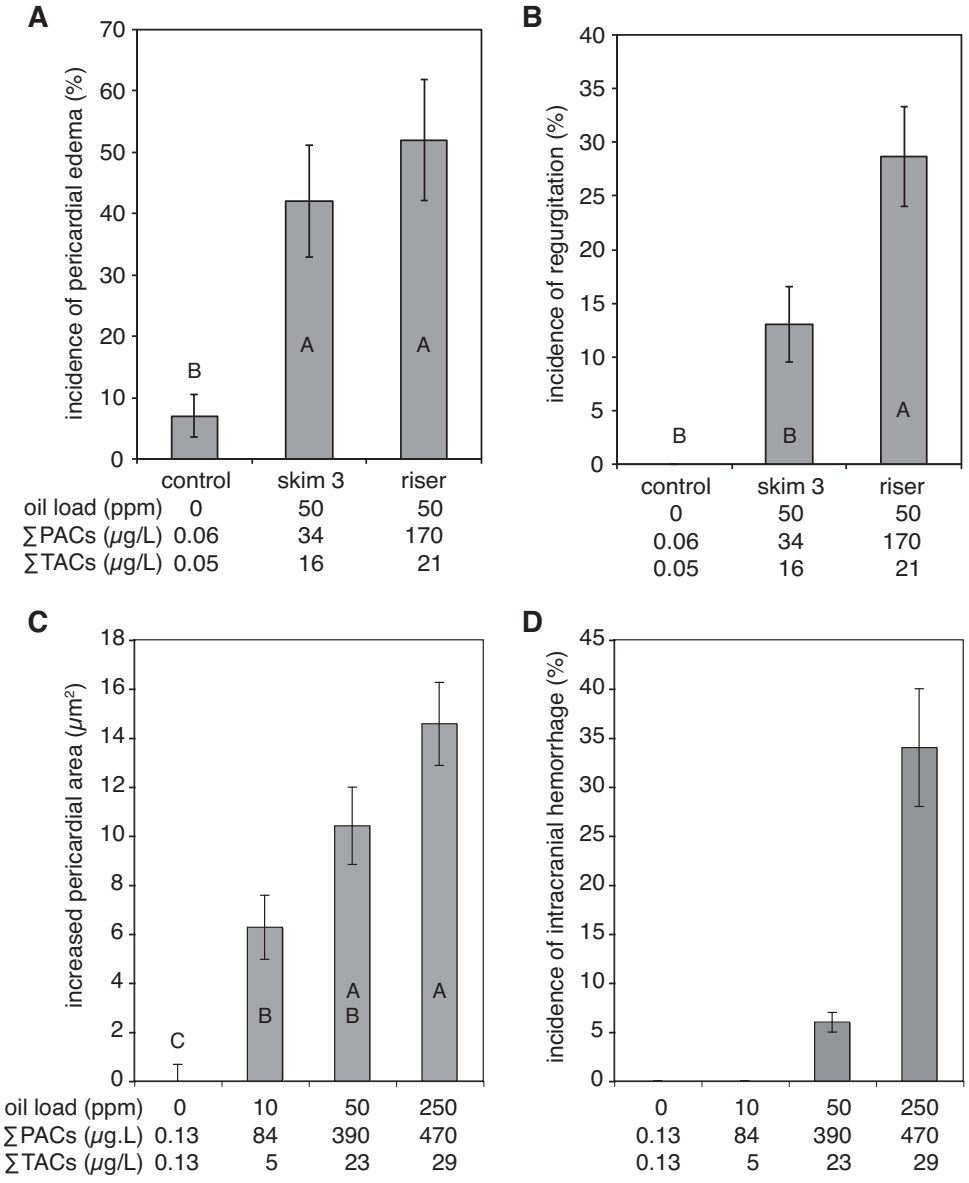

Fig. 5. Dose-dependent cardiovascular toxicity of MC252 riser oil. Embryos were exposed to filtered HEWAFS from 24 to 48 hpf (A, B) or unfiltered HEWAFs from 4 to 48 hpf (C, D). Data represent ~50 embryos total from three replicates for each treatment (means ± s.e.m. for $N = 3$). ANOVA was significant for effect of treatment for incidence of pericardial edema ($P = 0.02$) and regurgitation ($P = 0.003$) and nested ANOVA for pericardial area was significant for effect of treatment ($P < 0.001$). Statistically similar treatments are indicated by letters (post hoc test using Tukey–Kramer HSD, $\alpha = 0.05$). Statistical analysis was not applied to intracranial hemorrhage data. PAC values (μg/L) on the x-axis represent (A, B) measured total dissolved ∑PACs and total dissolved ∑TACs and (C, D) measured total dissolved plus particulate ∑PACs (top) and estimated dissolved ∑TACs (bottom).

epidermal cells scattered over the eye (Fig. 7A), with no CYP1A labeling in the heart (Fig. 7B). In contrast, exposure to MC252 riser oil resulted in strong CYP1A immunofluorescence throughout the entire epidermis, with a patchwork pattern of high and low levels in individual cells (Fig. 7C). CYP1A immunofluorescence was also observed in endothelial cells lining the heart (endocardium; Fig. 7D) but not in myocardial cells marked by myosin heavy chain immunofluorescence (Fig. 7D′ and D″). CYP1A induction was also

Table 3
Cardiac function in embryos exposed to MC252 crude oil from 24 to 48 hpf.

Cardiac measure	Control	Oil exposed	*P*-Value[a]
Atrial diastolic diameter (μm)	93.2 ± 3.6	100.2 ± 7.5	0.5
Atrial systolic diameter (μm)	64.6 ± 1.8	67.9 ± 3.4	0.4
Ventricular diastolic diameter (μm)	93.2 ± 1.8	76.0 ± 4.3	0.004
Ventricular systolic diameter (μm)	65.9 ± 2.5	61.8 ± 2.6	0.2
Atrial contractility (%)	29.9 ± 2.9	30.7 ± 2.9	1
Ventricular contractility (%)	29.3 ± 2.3	17.9 ± 2.3	0.003

[a] Cardiac measures were obtained from 3 to 4 digital videos from 3 treatment replicates (10 embryos total per treatment). Data were analyzed by ANOVA with replicate nested within treatment. *P*-Values shown are for effects of oil exposure. No measure showed an effect of replicate (e.g., "tank" effect; *P* values ranged from 0.11 to 0.73).

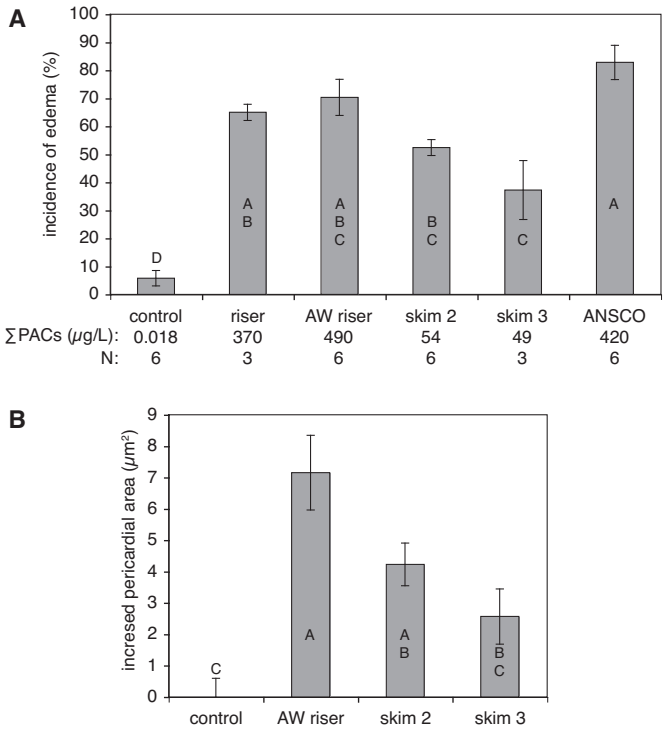

Fig. 6. Comparative cardiotoxicity of MC252 and ANSCO crude oils. Embryos were exposed to HEWAFs with 50 ppm nominal oil loads from 4 to 48 hpf and 15 to 20 embryos from each replicate were randomly selected for collection of lateral digital video clips. Incidence of edema (A) was scored by assessing each video clip, and still frames were generated to measure pericardial edema area (B). Data are mean ± s.e.m. for the given N (A), or for $N = 3$ (B). Data in A were derived from two independent experiments (that included artificially weathered [AW] riser, skim 2 and ANSCO) with three replicate groups each; data in B are from a single experiment. Nested ANOVAs were significant for effect of treatment ($P < 0.001$), and statistically similar treatments are indicated by letters (post hoc test using Tukey–Kramer HSD, $\alpha = 0.05$). PAC values are measured total dissolved and particulate.

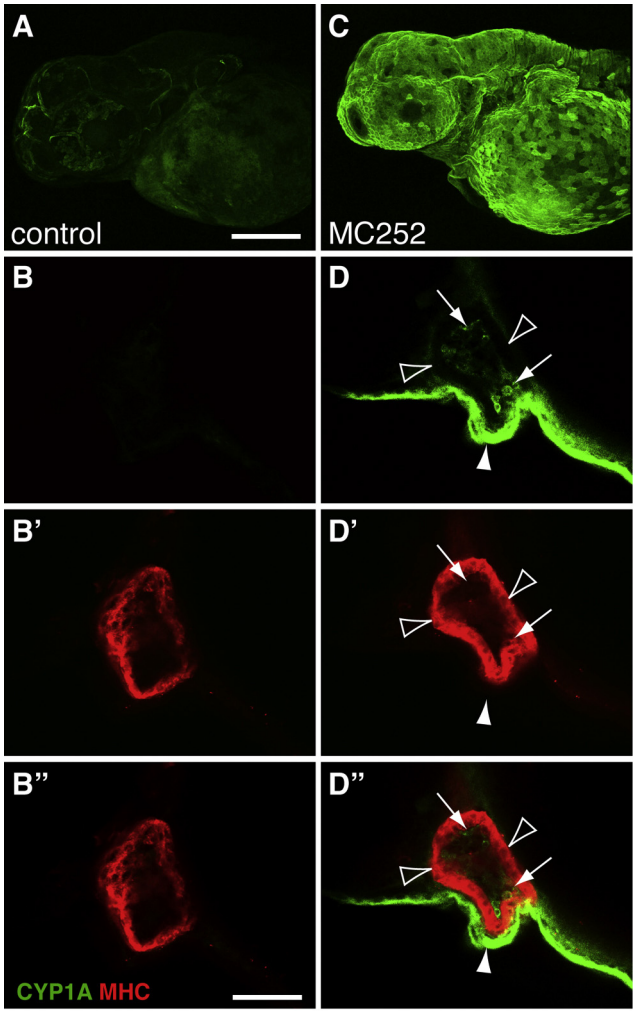

Fig. 7. CYP1A immunofluorescence in embryos exposed to MC252 riser oil. Embryos were exposed from 4 to 48 hpf, fixed and processed for CYP1A (green) and myosin heavy chain (red, marking cardiomyocytes) immunofluorescence. (A, B) Control embryos, (C, D) embryos exposed to MC252 riser HEWAF. (B, D) CYP1A immunofluorescence; (B′, D′) myosin heavy chain immunofluorescence; (B″, D″) merged image. Scale bars are 200 (A, C) and 50 μm (B, D). Filled arrowheads indicate CYP1A$^+$ epidermal cells, smaller arrows indicate CYP1A$^+$ endocardial cells, and unfilled arrowheads indicate myocardial cells lacking CYP1A immunofluorescence. Images are representative of ~20 embryos examined for each treatment.

evident in vascular endothelial cells throughout the trunk (not shown).

4. Discussion

The spawning seasons of many fish species in the northern Gulf of Mexico overlapped with the active crude oil release phase during the *Deepwater Horizon* incident, prior to the containment of the blown out MC252 wellhead (Arocha et al., 2001; Block et al., 2005; Grimes et al., 1990; Lang et al., 1994; McEachran et al., 1980; Murie and Parkyn, 2008; Rooker et al., 2012; Taylor et al., 2011; Teo et al., 2007; Thompson et al., 1991). Developing fish embryos were therefore likely to have been exposed to physically and chemically dispersed oil in the open Gulf, from the seafloor to sunlit surface waters, as well in contaminated marshes and other nearshore habitats. Exposure of zebrafish embryos to MC252 crude oil produced a familiar suite of abnormalities that includes cardiac dysfunction (e.g., reduced contractility) and dysmorphogenesis (e.g., defective looping), as well as finfold defects and intracranial hemorrhaging. Our side-by-side comparison of MC252 and Alaska North Slope crude oil embryotoxicity has thus shown that the former produces familiar types of cardiac injury, as elucidated by years of research on the latter (Incardona et al., 2012a; Peterson et al., 2003; Rice et al., 2001). The injury phenotype was consistent despite physical or chemical differences between MC252 and other crude oils, and the potency of artificially weathered MC252 oil was similar to artificially weathered ANSCO. Importantly, the zebrafish cardiac phenotype associated with MC252 oil exposure was nearly identical to that described previously (and confirmed here) for ANSCO (Incardona et al., 2005) as well as Iranian heavy crude oil (Jung et al., 2013). Each of these three geologically distinct crude oils specifically reduced diastolic relaxation of the ventricle, impairing its contractility and resulting in poor cardiac looping.

The relative sensitivity of zebrafish embryos to crude oil toxicity compared to marine embryos indigenous to the Gulf of Mexico is unknown. However, although the ∑PAC concentrations producing severe cardiotoxicity tested here are at least 10-times higher than those that produce similar effects in temperate species such as Pacific herring (Incardona et al., 2012b), they are in the range of levels detected during the Deepwater Horizon incident (e.g., up to ∑PACs 189 μg/L; Diercks et al., 2010). While cold-water species such as herring and salmon have been intensively studied, there is little information on how the higher temperatures of the Gulf of Mexico (e.g., 25–28 °C) might modify PAC bioavailability and crude oil toxicity. However, our findings with tropical zebrafish cultured at 28 °C suggest that the higher temperatures in the Gulf would not mitigate MC252 cardiotoxicity in fish embryos.

The steady release of oil under high pressure, together with the application of dispersant at the damaged wellhead, led to formation of large subsurface plumes of oil droplets (Adcroft et al., 2010; Camilli et al., 2010; North et al., 2011). We have developed a simple experimental approach to produce aqueous suspensions of small oil droplets. This high energy WAF method can be used in subsequent studies to systematically assess the toxicity of MC252 crude oil to embryos of native Gulf fishes and other open water organisms. For both unweathered MC252 riser oil and more viscous surface slick samples, the blender method generated high-energy WAFs with highly reproducible and consistent oil droplet sizes and PAC compositions in both dissolved and particulate fractions. Overall droplet diameters were toward the lower end of the environmentally relevant size range for droplets that formed subsurface plumes during the *Deepwater Horizon* spill (10–50 μm (North et al., 2011)). While PAC measurements are essential to any systematic toxicity testing program, the high reproducibility of the blender HEWAF method has the potential to reduce costs by providing consistent dissolved PAC concentrations based on nominal oil loads.

Although the precise compounds responsible for phototoxicity remain unknown (Barron and Ka'aihue, 2001; Hatlen et al., 2010), ANSCO and MC252 crude oils produced morphologically indistinguishable photosensitization reactions with a severity that correlated with nominal dosing predicted to produce ANSCO and MC252 skim 1 HEWAFs with comparable aqueous PAC concentrations, based on the measured PAC concentrations in each of these oil samples. Lethal phototoxicity has recently been documented in marine fish embryos following a spill of more toxicologically potent residual fuel oil in the turbid waters of San Francisco Bay (Incardona et al., 2012a, 2012b), and our current findings indicate a potential for phototoxic effects of MC252 oil in the comparatively translucent sunlit surface waters of the Gulf of Mexico.

The morphological and functional defects following continuous exposure to MC252 oil HEWAFs starting near the beginning of gastrulation (~4 hpf) up to 48 hpf (early hatching stage) were virtually indistinguishable from those caused by ANSCO exposure (Incardona et al., 2005), with patterns of CYP1A induction nearly identical for both oil types. At the same time, exposures starting after initial formation of a functional heart tube (e.g., 24 hpf) produced the same defects in heart looping and contractility as those observed for exposures that began shortly after fertilization (e.g., 4–6 hpf). In either case, we observed no novel forms of developmental toxicity in response to MC252 oil exposures. The cardiotoxic effects of unweathered and weathered MC252 oil samples were largely the same, and these oil samples differed primarily in potency when considered on the basis of total PAC content. Consequently, the toxicity of unweathered MC252 riser oil was comparable to weathered samples (e.g., skim 3) despite very different $\sum$PAC concentrations, due to the much larger fraction of naphthalenes in the former. These findings are consistent with a wealth of data on ANSCO showing that toxicity based on units of $\sum$PAC increases with weathering as the relative proportion of the tricyclic PACs increases and naphthalenes are lost (e.g., Carls et al., 1999; Heintz et al., 1999).

Our findings also provide further evidence for a gradient of oil exposure phenotypes in developing teleost fish that are concentration-dependent and fall into three broad categories: (1) defects in cardiac form and function (i.e., cardiotoxicity), (2) defects in other tissues that are secondary to reduced cardiac function, and (3) cardiac-independent defects. At the high end of the gradient, irreversible heart failure leads to a cascade of effects secondary to loss of circulation, resulting in severe edema, craniofacial abnormalities, and in some cases body axis distortion. These defects occur in parallel with cardiac-independent intracranial hemorrhages and finfold defects (Incardona et al., 2004, 2005; Jung et al., 2013). At this higher end of the gradient, affected fish have jaw deformities and reduced swimming that preclude feeding, and they die as larvae (present results; Hicken et al., 2011). At the low end of the severity gradient, embryos display only subtle cardiotoxic effects, as evidenced in this study by mild edema at the hatching stage (48 hpf). These fish survive as larvae in a laboratory husbandry facility, and they subsequently appear outwardly normal. However, fluid accumulation around the heart during embryonic development is an indicator of disrupted cardiovascular function during a critical window of cardiac morphogenesis. The formation of the fish heart follows function (Glickman and Yelon, 2002; Schoenebeck and Yelon, 2007), and it has been previously shown that oil-exposed zebrafish survive to adulthood albeit with permanent changes to the shape of the heart that reduce swimming performance (Hicken et al., 2011). Under natural conditions, these types of permanent effects would likely reduce fish survival at juvenile, subadult, or adult life stages. Overall, cardiac morphogenesis is the most sensitive and diagnostic indicator of injury in fish embryos exposed to relatively low levels of crude oil, including MC252 crude.

A recent investigation reported similar gross phenotypes in zebrafish embryos and larvae exposed to much higher concentrations of MC252 riser oil WAF prepared by a different method (de Soysa et al., 2012). Severely affected embryos were evaluated at later stages of development (up to 5 dpf) than for this study. Several potentially novel phenotypes were identified, including abnormal locomotor responses. Notably, a phenotype displaying variable reduction in posterior elements of the craniofacial cartilages (ceratobranchials 5–7) was also observed. This was attributed to a similarly variable reduction in migratory neural crest cells that give rise to posterior arches (Schilling and Kimmel, 1994), suggesting by extension that MC252 oil-induced cardiac defects were caused by a reduction in neural crest cells that migrate from the pharyngeal arches and differentiate into cardiomyocytes (de Soysa et al., 2012). In zebrafish, the cells that give rise to cardiomyocytes come from two general populations during two periods of development. The first source is the primary heart field during the initial development of the primitive heart tube (16–24 hpf) (Yelon et al., 1999), followed by cells from the secondary heart field during later maturation of the ventricle and outflow tract (24–60 hpf) (Hami et al., 2011; Lazic and Scott, 2011; Zhou et al., 2011). The primary heart field, a bilateral region of cells in the anterior lateral plate mesoderm, provides myocardial precursors to the forming atrium and ventricle (Glickman and Yelon, 2002; Yelon et al., 1999). In a process that distinguishes zebrafish from other vertebrates, neural crest cells also migrate from the adjacent pharyngeal arches and contribute to the cell population of the primary heart field (Li et al., 2003; Sato and Yost, 2003). Embryos in which neural crest cells are ablated or fail to migrate or differentiate due to genetic loss-of-function display a cardiac phenotype that is superficially similar to the crude oil injury phenotype (e.g., imperfect looping, reduced contractility and heart rate (Li et al., 2003; Sato et al., 2006)). Notably, neural crest cell migration to the primary heart field occurs between the 16- and 22-somite stages (~16–19 hpf) (Sato et al., 2006). In the current study we find (1) conventional cardiotoxicity following exposures that began after this developmental window (24–48 hpf) and (2) normal craniofacial development in juveniles that displayed cardiotoxicity (edema) at 48 hpf. Together, these results rule out perturbed cardiac neural crest migration as the underlying mechanism for the observed defects in heart form and function in response to the much lower MC252 crude oil exposure concentrations used in this study, or in previous studies using other crude oils.

The absence of intracranial hemorrhage in embryos exposed during the 24–48 hpf developmental window provides some insight into the etiology of this defect. Although blood–brain barrier formation occurs after 48 hpf in zebrafish (Jeong et al., 2008), a key period of cerebrovascular stabilization spanning 36–52 hpf was revealed by analyses of zebrafish vascular mutants *bubblehead* and

redhead (Buchner et al., 2007; Liu et al., 2007). Oil exposures prior to 24 hpf are necessary to produce hemorrhaging; however, hemorrhages appear later in the same ontogenetic window as for *bubblehead* and *redhead* mutants. Similar to these two mutants, the vessels of crude oil-exposed embryos appear to undergo repair after hemorrhage occurs. Molecular analyses of these mutants and additional morpholino knockdown studies revealed a cerebrovascular stabilization pathway that involves βPix, a guanine nucleotide exchange factor for Rac and Cdc42, its binding partner p21-activated kinase 2 (Pak2), integrin $\alpha_v\beta_8$, and A-kinase anchoring protein 12 (AKAP12) (Buchner et al., 2007; Kwon et al., 2012; Liu et al., 2007, 2012). Similar hemorrhages occur in the same developmental period with exposure to high molecular weight PACs containing four or more rings that are potent agonists of the aryl hydrocarbon receptor (AHR) (Incardona et al., 2006, 2011), but these compounds are typically present only at very low concentrations, or are absent, in crude oil HEWAFs. It is unclear whether hemorrhaging is AHR-mediated in HEWAF-exposed embryos, because AHR knockdown exacerbated oil-induced cardiac defects, and embryos with reduced circulation did not exhibit hemorrhage (Incardona et al., 2005). Nevertheless, the p21-activated kinase/integrin pathway could be a direct or indirect target (e.g., downstream of AHR activation) of as-yet unidentified crude oil compounds.

Reductions of finfold outgrowth and finfold malformations are common among embryos exposed to different crude oils, including MC252, ANSCO (Incardona et al., 2005) and Iranian heavy crude (Jung et al., 2013). Similar finfold phenotypes have also been documented in a number of zebrafish mutants and morphants, providing a possible indication of the underpinning molecular pathways for this form of crude oil toxicity. These include the mutants *pinfin*, *blasen*, *rafels* and *sturgeon*. With the exception of *sturgeon*, all involve mutations in extracellular matrix (ECM) genes. In particular, the Fras1/Frem complex in *pinfin*, *blasen*, and *rafels* is disrupted, resulting in a reduced basement membrane – i.e., dermis attachment in the developing finfold (Carney et al., 2010). This leads to blisters resembling those observed in older (e.g., 72 hpf) oil-exposed embryos (Incardona et al., 2005). A similar phenotype was observed in the *sturgeon* mutant, which disrupts furinA, a proprotein convertase necessary for proteolytic cleavage of Fras1/Frem proteins from the cell surface into the finfold basement membrane (Carney et al., 2010). Outgrowth of the finfold is dependent on actinotrichia, non-calcified skeletal elements that are visible as brush-like rays in the caudal finfold. Actinotrichia require collagen type I and II isoforms that are encoded by *col1a1a* and *col2a1b* genes. Knockdown of the latter produced a much more severe loss of finfolds, while *col1a1* knockdown resulted in a phenotype of shorter actinotrichia and reduced caudal finfold outgrowth that is very similar to the effects of oil exposure (Duran et al., 2011). Furins are also known to target collagens among other fin morphogenesis proteins in addition to the Fras1/Frem complex (Lehmann et al., 1996; Veit et al., 2007). Therefore, a reduced finfold outgrowth in response to crude oil exposure could result from direct effects on any of these ECM structural elements or through effects on furin-dependent post-translational processing. The chemical etiology is not well defined to date because individual PACs evaluated as single compounds do not produce similar finfold defects (Incardona et al., 2004, 2005, 2006, 2011; Scott et al., 2011).

The *Exxon Valdez* spill had long-lasting ecosystem impacts on neritic and pelagic habitats in Prince William Sound, causing increased mortality in developing pink salmon for several years after the spill (Rice et al., 2001). Other species were affected to varying degrees (Peterson, 2001), and the *Exxon Valdez* disaster may have caused the population-scale collapse of Pacific herring (Thorne and Thomas, 2008). A large number of studies on ANSCO in the years following the *Exxon Valdez* spill yielded a wealth of insights into the acute and long-term effects of crude oil on fish early life stages and pinpointed the cardiovascular system as the major point of injury. Using the zebrafish model as a bridge species, we have shown that MC252 oil and ANSCO are substantively similar in terms of canonical crude oil toxicity to embryos and larvae. While many aspects of the etiology of impact in a warm water environment (Gulf of Mexico) remain unknown, the established literature can inform resource managers and others working to assess year-class losses of marine fish species that spawned in the northern Gulf of Mexico during and after the *Deepwater Horizon* incident. Importantly, a much greater diversity of teleost fishes use this subtropical spawning habitat relative to fish assemblages spawning in the much colder waters of Prince William Sound. A renewed focus on crude oil toxicity in the aftermath of the largest spill in U.S. history will extend the insights gained following the *Exxon Valdez* spill. Specifically, new research will likely spur discoveries into the precise mechanisms by which tricyclic PACs disrupt cardiac function and development in fish. This in turn will improve the scientific basis for diagnosing oil exposure and injury, thereby informing future environmental surveillance efforts.

Acknowledgements

We thank Heather Day for technical assistance during early phases of this work, Gina Ylitalo for discussions about PAC analytical chemistry, Mark Carls for discussions on developing a high-energy HEWAF protocol and critical review of the manuscript, and Jeff Morris and Ryan Takeshita for critical reviews of the manuscript. This work was funded as a contributing study to the Deepwater Horizon – MC252 Incident Natural Resource Damage Assessment.

References

Adcroft, A., Hallberg, R., Dunne, J.P., Samuels, B.L., Galt, J.A., Barker, C.r.H., Payton, D., 2010. Simulations of underwater plumes of dissolved oil in the Gulf of Mexico. Geophys. Res. Lett. 37, L18605.

Arocha, F., Lee, D.W., Marcano, L.A., Marcano, J.S., 2001. Update information on the spawning of yellowfin tuna, *Thunnus albacares*, in the western central Atlantic. Col. Vol. Sci. Pap., ICCAT 52, 167–176.

Barron, M.G., Carls, M.G., Short, J.W., Rice, S.D., 2003. Photoenhanced toxicity of aqueous phase and chemically dispersed weathered Alaska North Slope crude oil to Pacific herring eggs and larvae. Environ. Toxicol. Chem. 22, 650–660.

Barron, M.G., Ka'aihue, L., 2001. Potential for photoenhanced toxicity of spilled oil in Prince William Sound and Gulf of Alaska Waters. Mar. Pollut. Bull. 43, 86–92.

Bendig, G., Grimmler, M., Huttner, I.G., Wessels, G., Dahme, T., Just, S., Trano, N., Katus, H.A., Fishman, M.C., Rottbauer, W., 2006. Integrin-linked kinase, a novel component of the cardiac mechanical stretch sensor, controls contractility in the zebrafish heart. Genes Dev. 20, 2361–2372.

Block, B.A., Teo, S.L.H., Walli, A., Boustany, A., Stokesbury, M.J.W., Farwell, C.J., Weng, K.C., Dewar, H., Williams, T.D., 2005. Electronic tagging and population structure of Atlantic bluefin tuna. Nature 434, 1121–1127.

Buchner, D.A., Su, F., Yamaoka, J.S., Kamei, M., Shavit, J.A., Barthel, L.K., McGee, B., Amigo, J.D., Kim, S., Hanosh, A.W., Jagadeeswaran, P., Goldman, D., Lawson, N.D., Raymond, P.A., Weinstein, B.M., Ginsburg, D., Lyons, S.E., 2007. pak2a mutations cause cerebral hemorrhage in redhead zebrafish. Proc. Natl. Acad. Sci. U.S.A. 104, 13996–14001.

Camilli, R., Reddy, C.M., Yoerger, D.R., Van Mooy, B.A.S., Jakuba, M.V., Kinsey, J.C., McIntyre, C.P., Sylva, S.P., Maloney, J.V., 2010. Tracking hydrocarbon plume transport and biodegradation at Deepwater Horizon. Science 330, 201–204.

Carls, M.G., Holland, L., Larsen, M., Collier, T.K., Scholz, N.L., Incardona, J.P., 2008. Fish embryos are damaged by dissolved PAHs, not oil particles. Aquat. Toxicol. 88, 121–127.

Carls, M.G., Meador, J.P., 2009. A perspective on the toxicity of petrogenic PAHs to developing fish embryos related to environmental chemistry. Hum. Ecol. Risk Assess. 15, 1084–1098.

Carls, M.G., Rice, S.D., Hose, J.E., 1999. Sensitivity of fish embryos to weathered crude oil: Part I. Low-level exposure during incubation causes malformations, genetic damage, and mortality in larval Pacific herring (*Clupea pallasi*). Environ. Toxicol. Chem. 18, 481–493.

Carney, T.J., Feitosa, N.M., Sonntag, C., Slanchev, K., Kluger, J., Kiyozumi, D., Gebauer, J.M., Coffin Talbot, J., Kimmel, C.B., Sekiguchi, K., Wagener, R., Schwarz, H., Ingham, P.W., Hammerschmidt, M., 2010. Genetic analysis of fin development in zebrafish identifies furin and hemicentin1 as potential novel fraser syndrome disease genes. PLoS Genet. 6, e1000907.

Chi, N.C., Shaw, R.M., Jungblut, B., Huisken, J., Ferrer, T., Arnaout, R., Scott, I.C., Beis, D., Xiao, T., Baier, H., Jan, L.Y., Tristani-Firouzi, M., Stainier, D.Y.R., 2008. Genetic

and physiologic dissection of the vertebrate cardiac conduction system. PLoS Biol. 6, e109.
Couillard, C.M., 2002. A microscale test to measure petroleum oil toxicity to mummichog embryos. Environ. Toxicol. 17, 195–202.
Couillard, C.M., Lee, K., Legare, B., King, T.L., 2005. Effect of dispersant on the composition of the water-accommodated fraction of crude oil and its toxicity to larval marine fish. Environ. Toxicol. Chem. 24, 1496–1504.
Council, N.R., 2003. Oil in the Sea III: Inputs, Fates, and Effects. National Research Council, Washington, DC, pp. 446.
de Soysa, T.Y., Ulrich, A., Friedrich, T., Pite, D., Compton, S.L., Ok, D., Bernardos, R.L., Downes, G.B., Hsieh, S., Stein, R., Lagdameo, M.C., Halvorsen, K., Kesich, L.R., Barresi, M.J., 2012. Macondo crude oil from the Deepwater Horizon oil spill disrupts specific developmental processes during zebrafish embryogenesis. BMC Biol. 10, 40.
Diercks, A.-R., Highsmith, R.C., Asper, V.L., Joung, D., Zhou, Z., Guo, L., Shiller, A.M., Joye, S.B., Teske, A.P., Guinasso, N., Wade, T.L., Lohrenz, S.E., 2010. Characterization of subsurface polycyclic aromatic hydrocarbons at the Deepwater Horizon site. Geophys. Res. Lett. 37, L20602.
Duran, I., Mari-Beffa, M., Santamaria, J.A., Becerra, J., Santos-Ruiz, L., 2011. Actinotrichia collagens and their role in fin formation. Dev. Biol. 354, 160–172.
Glickman, N.S., Yelon, D., 2002. Cardiac development in zebrafish: coordination of form and function. Semin. Cell Dev. Biol. 13, 507–513.
Grimes, C.B., Finucane, J.H., Collins, A.L., DeVries, D.A., 1990. Young King Mackerel, Scomberomorus Cavalla, in the Gulf of Mexico, a summary of the distribution and occurrence of larvae and juveniles, and spawning dates for Mexican juveniles. Bull. Mar. Sci. 46, 640–654.
Hami, D., Grimes, A.C., Tsai, H.J., Kirby, M.L., 2011. Zebrafish cardiac development requires a conserved secondary heart field. Development 138, 2389–2398.
Hatlen, K., Sloan, C.A., Burrows, D.G., Collier, T.K., Scholz, N.L., Incardona, J.P., 2010. Natural sunlight and residual fuel oils are an acutely lethal combination for fish embryos. Aquat. Toxicol. 99, 56–64.
Heintz, R.A., 2007. Chronic exposure to polynuclear aromatic hydrocarbons in natal habitats leads to decreased equilibrium size, growth, and stability of pink salmon populations. Integr. Environ. Assess. Manag. 3, 351–363.
Heintz, R.A., Short, J.W., Rice, S.D., 1999. Sensitivity of fish embryos to weathered crude oil: Part II. Increased mortality of pink salmon (*Oncorhynchus gorbuscha*) embryos incubating downstream from weathered Exxon Valdez crude oil. Environ. Toxicol. Chem. 18, 494–503.
Hicken, C.E., Linbo, T.L., Baldwin, D.H., Willis, M.L., Myers, M.S., Holland, L., Larsen, M., Stekoll, M.S., Rice, G.S., Collier, T.K., Scholz, N.L., Incardona, J.P., 2011. Sub-lethal exposure to crude oil during embryonic development alters cardiac morphology and reduces aerobic capacity in adult fish. Proc. Natl. Acad. Sci. U.S.A. 108, 7086–7090.
Incardona, J.P., Carls, M.G., Day, H.L., Sloan, C.A., Bolton, J.L., Collier, T.K., Scholz, N.L., 2009. Cardiac arrhythmia is the primary response of embryonic Pacific herring (*Clupea pallasi*) exposed to crude oil during weathering. Environ. Sci. Technol. 43, 201–207.
Incardona, J.P., Carls, M.G., Teraoka, H., Sloan, C.A., Collier, T.K., Scholz, N.L., 2005. Aryl hydrocarbon receptor-independent toxicity of weathered crude oil during fish development. Environ. Health Perspect. 113, 1755–1762.
Incardona, J.P., Collier, T.K., Scholz, N.L., 2004. Defects in cardiac function precede morphological abnormalities in fish embryos exposed to polycyclic aromatic hydrocarbons. Toxicol. Appl. Pharmacol. 196, 191–205.
Incardona, J.P., Day, H.L., Collier, T.K., Scholz, N.L., 2006. Developmental toxicity of 4-ring polycyclic aromatic hydrocarbons in zebrafish is differentially dependent on AH receptor isoforms and hepatic cytochrome P450 1A metabolism. Toxicol. Appl. Pharmacol. 217, 308–321.
Incardona, J.P., Linbo, T.L., Scholz, N.L., 2011. Cardiac toxicity of 5-ring polycyclic aromatic hydrocarbons is differentially dependent on the aryl hydrocarbon receptor 2 isoform during zebrafish development. Toxicol. Appl. Pharmacol. 257, 242–249.
Incardona, J.P., Vines, C.A., Anulacion, B.F., Baldwin, D.H., Day, H.L., French, B.L., Labenia, J.S., Linbo, T.L., Myers, M.S., Olson, O.P., Sloan, C.A., Sol, S., Griffin, F.J., Menard, K., Morgan, S.G., West, J.E., Collier, T.K., Ylitalo, G.M., Cherr, G.N., Scholz, N.L., 2012a. Unexpectedly high mortality in Pacific herring embryos exposed to the 2007 Cosco Busan oil spill in San Francisco Bay. Proc. Natl. Acad. Sci. U.S.A. 109, E51–E58.
Incardona, J.P., Vines, C.A., Linbo, T.L., Myers, M.S., Sloan, C.A., Anulacion, B.F., Boyd, D., Collier, T.K., Morgan, S., Cherr, G.N., Scholz, N.L., 2012b. Potent phototoxicity of marine bunker oil to translucent herring embryos after prolonged weathering. PLoS ONE 7, e30116.
Jeong, J.Y., Kwon, H.B., Ahn, J.C., Kang, D., Kwon, S.H., Park, J.A., Kim, K.W., 2008. Functional and developmental analysis of the blood–brain barrier in zebrafish. Brain Res. Bull. 75, 619–628.
Jung, J.-H., Hicken, C.E., Boyd, D., Anulacion, B.F., Carls, M.G., Shim, W.J., Incardona, J.P., 2013. Geologically distinct crude oils cause a common cardiotoxicity syndrome in developing zebrafish. Chemosphere 91, 1146–1155.
Kwon, H.B., Choi, Y.K., Lim, J.J., Kwon, S.H., Her, S., Kim, H.J., Lim, K.J., Ahn, J.C., Kim, Y.M., Bae, M.K., Park, J.A., Jeong, C.H., Mochizuki, N., Kim, K.W., 2012. AKAP12 regulates vascular integrity in zebrafish. Exp. Mol. Med. 44, 225–235.
Lang, K.L., Grimes, C.B., Shaw, R.F., 1994. Variations in the age and growth of yellowfin tuna larvae, *Thunnus albacares*, collected about the Mississippi River plume. Environ. Biol. Fishes 39, 259–270.
Lazic, S., Scott, I.C., 2011. Mef2cb regulates late myocardial cell addition from a second heart field-like population of progenitors in zebrafish. Dev. Biol. 354, 123–133.
Lehmann, M., Rigot, V., Seidah, N.G., Marvaldi, J., Lissitzky, J.C., 1996. Lack of integrin alpha-chain endoproteolytic cleavage in furin-deficient human colon adenocarcinoma cells LoVo. Biochem. J. 317 (Pt 3), 803–809.
Li, Y.X., Zdanowicz, M., Young, L., Kumiski, D., Leatherbury, L., Kirby, M.L., 2003. Cardiac neural crest in zebrafish embryos contributes to myocardial cell lineage and early heart function. Dev. Dyn. 226, 540–550.
Linbo, T.L., 2009. Zebrafish (*Danio rerio*) husbandry and colony maintenance at the Northwest Fisheries Science Center. NOAA Technical Memorandum. U.S. Department of Commerce, pp. 75.
Liu, J., Fraser, S.D., Faloon, P.W., Rollins, E.L., Vom Berg, J., Starovic-Subota, O., Laliberte, A.L., Chen, J.-N., Serluca, F.C., Childs, S.J., 2007. A βPix-Pak2a signaling pathway regulates cerebral vascular stability in zebrafish. Proc. Natl. Acad. Sci. U.S.A. 104, 13990–13995.
Liu, J., Zeng, L., Kennedy, R.M., Gruenig, N.M., Childs, S.J., 2012. beta Pix plays a dual role in cerebral vascular stability and angiogenesis, and interacts with integrin alpha(v)beta(8). Dev. Biol. 363, 95–105.
Marty, G.D., Hose, J.E., McGurk, M.D., Brown, E.D., Hinton, D.E., 1997a. Histopathology and cytogenetic evaluation of Pacific herring larvae exposed to petroleum hydrocarbons in the laboratory or in Prince William Sound, Alaska, after the Exxon Valdez oil spill. Can. J. Fish. Aquat. Sci. 54, 1846–1857.
Marty, G.D., Short, J.W., Dambach, D.M., Willits, N.H., Heintz, R.A., Rice, S.D., Stegeman, J.J., Hinton, D.E., 1997b. Ascites, premature emergence, increased gonadal cell apoptosis, and cytochrome P4501A induction in pink salmon larvae continuously exposed to oil-contaminated gravel during development. Can. J. Zool. Rev. Can. Zool. 75, 989–1007.
McEachran, J.D., Finucane, J.H., Hall, L.S., 1980. Distribution, seasonality and abundance of king and Spanish mackerel larvae in the northwestern Gulf of Mexico (Pisces: Scombridae). Northeast Gulf Sci. 4, 1–16.
Murie, D.J., Parkyn, D.C., 2008. Age, growth and sex maturity of greater amberjack (*Seriola dumerili*) in the Gulf of Mexico. Marine Fisheries Research Initiative (MARFIN) Program, Final Report. National Marine Fisheries Service, St. Petersburg, FL.
North, E.W., Adams, E.E., Schlag, Z., Sherwood, C.R., He, R., Hyun, K.H., Socolofsky, S.A., 2011. Simulating Oil Droplet Dispersal from the Deepwater Horizon Spill with a Lagrangian Approach. Monitoring and Modeling the Deepwater Horizon Oil Spill: A Record-Breaking Enterprise, vol. 195. AGU, Washington, DC, pp. 217–226.
Peterson, C.H., 2001. The "Exxon Valdez" oil spill in Alaska: acute, indirect and chronic effects on the ecosystem. Adv. Mar. Biol. 39, 1–103.
Peterson, C.H., Rice, S.D., Short, J.W., Esler, D., Bodkin, J.L., Ballachey, B.E., Irons, D.B., 2003. Long-term ecosystem response to the Exxon Valdez oil spill. Science 302, 2082–2086.
Pollino, C.A., Holdway, D.A., 2002. Toxicity testing of crude oil and related compounds using early life stages of the crimson-spotted rainbowfish (*Melanotaenia fluviatilis*). Ecotox. Environ. Saf. 52, 180–189.
Rice, S.D., Thomas, R.E., Carls, M.G., Heintz, R.A., Wertheimer, A.C., Murphy, M.L., Short, J.W., Moles, A., 2001. Impacts to pink salmon following the Exxon Valdez oil spill: Persistence, toxicity, sensitivity, and controversy. Rev. Fish. Sci. 9, 165–211.
Rooker, J.R., Simms, J.R., Wells, R.J.D., Holt, S.A., Holt, G.J., Graves, J.E., Furey, N.B., 2012. Distribution and habitat associations of billfish and swordfish larvae across mesoscale features in the Gulf of Mexico. PLoS One 7, e34180.
Sato, M., Tsai, H.J., Yost, H.J., 2006. Semaphorin3D regulates invasion of cardiac neural crest cells into the primary heart field. Dev. Biol. 298, 12–21.
Sato, M., Yost, H.J., 2003. Cardiac neural crest contributes to cardiomyogenesis in zebrafish. Dev. Biol. 257, 127–139.
Schilling, T.F., Kimmel, C.B., 1994. Segment and cell type lineage restrictions during pharyngeal arch development in the zebrafish embryo. Development 120, 483–494.
Schoenebeck, J.J., Yelon, D., 2007. Illuminating cardiac development: advances in imaging add new dimensions to the utility of zebrafish genetics. Semin. Cell Dev. Biol. 18, 27–35.
Scott, J.A., Incardona, J.P., Pelkki, K., Shepardson, S., Hodson, P.V., 2011. AhR2-mediated; CYP1A-independent cardiovascular toxicity in zebrafish (*Danio rerio*) embryos exposed to retene. Aquat. Toxicol. 101, 165–174.
Singer, M.M., Aurand, D., Bragin, G.E., Clark, J.R., Coelho, G.M., Sowby, M.L., Tjeerdema, R.S., 2000. Standardization of the preparation and quantitation of water-accommodated fractions of petroleum for toxicity testing. Mar. Pollut. Bull. 40, 1007–1016.
Sloan, C.A., Brown, D.W., Pearce, R.W., Boyer, R.H., Bolton, J.L., Burrows, D.G., Herman, D.P., Krahn, M.M., 2005. Determining aromatic hydrocarbons and chlorinated hydrocarbons in sediments and tissues using accelerated solvent extraction and gas chromatography/mass spectrometry. In: Ostrander, G.K. (Ed.), Techniques in Aquatic Toxicology, vol. 2. CRC Press, Boca Raton, FL, pp. 631–651.
Stout, S.A., Wang, Z., 2007. Chemical fingerprinting of spilled or discharged petroleum - Methods and factors affecting petroleum fingerprints in the environment. In: Wang, Z., Stout, S.A. (Eds.), Oil Spill Environmental Forensics. Academic Press, London, pp. 1–53.
Taylor, N.G., McAllister, M.K., Lawson, G.L., Carruthers, T., Block, B.A., 2011. Atlantic Bluefin Tuna: a novel multistock spatial model for assessing population biomass. PLoS One 6, e27693.
Teo, S., Boustany, A., Dewar, H., Stokesbury, M., Weng, K., Beemer, S., Seitz, A., Farwell, C., Prince, E., Block, B., 2007. Annual migrations, diving behavior, and thermal biology of Atlantic bluefin tuna, *Thunnus thynnus*, on their Gulf of Mexico breeding grounds. Mar. Biol. 151, 1–18.

Thompson, B.A., Wilson, C.A., Render, J.H., Beasley, M., Cauthron, C., 1991. Age, growth, and reproductive biology of greater amberjack and cobia from Louisiana waters. Marine Fisheries Research Initiative (MARFIN) Program, Final Report. National Marine Fisheries Service, St. Petersburg, FL.

Thorne, R.E., Thomas, G.L., 2008. Herring and the "Exxon Valdez" oil spill: an investigation into historical data conflicts. ICES J. Mar. Sci. 65, 44–50.

Veit, G., Zimina, E.P., Franzke, C.W., Kutsch, S., Siebolds, U., Gordon, M.K., Bruckner-Tuderman, L., Koch, M., 2007. Shedding of collagen XXIII is mediated by furin and depends on the plasma membrane microenvironment. J. Biol. Chem. 282, 27424–27435.

Wang, Z., Hollebone, B.P., Fingas, M., Fieldhouse, B., Sigouin, L., Landriault, M., Smith, P., Noonan, J., Thouin, G., Weaver, J.W., 2003. Characteristics of spilled oils, fuels, and petroleum products: 1. Composition and properties of selected oils. U.S. Environmental Protection Agency, Washington, DC.

Yelon, D., Horne, S.A., Stainier, D.Y., 1999. Restricted expression of cardiac myosin genes reveals regulated aspects of heart tube assembly in zebrafish. Dev. Biol. 214, 23–37.

Zhou, Y., Cashman, T.J., Nevis, K.R., Obregon, P., Carney, S.A., Liu, Y., Gu, A., Mosimann, C., Sondalle, S., Peterson, R.E., Heideman, W., Burns, C.E., Burns, C.G., 2011. Latent TGF-beta binding protein 3 identifies a second heart field in zebrafish. Nature 474, 645–648.